International Immunopharmacology 120 (2023) 110408

Contents lists available at ScienceDirect

International Immunopharmacology

journal homepage: www.elsevier.com/locate/intimp

Ginsenoside Rg5 alleviates Ang II–induced cardiac inflammation and remodeling by inhibiting the JNK/AP-1 pathway

Tianxiang Yu [a,b,1], Xiangwei Xu [a,1], Jiajia Wei [d], Jiachen Xu [b], Wu Luo [b,c], Ankang Li [a], Guang Liang [a,b,*], Mengyang Wang [a,b,e,*]

[a] Affiliated Yongkang First People's Hospital and School of Pharmacy, Hangzhou Medical College, Hangzhou, Zhejiang 310012, China
[b] Chemical Biology Research Center, School of Pharmaceutical Sciences, Wenzhou Medical University, Wenzhou, Zhejiang 325035, China
[c] Department of Cardiology and Medical Research Center, The First Affiliated Hospital, Wenzhou Medical University, Wenzhou, Zhejiang 325035, China
[d] Zhejiang Provincial Key Laboratory of Laboratory Animals and Safety Research, Hangzhou Medical College, Hangzhou, China
[e] Key Laboratory of Natural Medicines of the Changbai Mountain, Ministry of Education, Yanbian University, Yanji 133002, China

ARTICLE INFO

Keywords:
Angiotensin II
Ginsenoside Rg5
c-Jun N-terminal kinase
Inflammation
Hypertensive heart failure

ABSTRACT

Increased level of Angiotensin II (Ang II) contributes to hypertensive heart failure via -hemodynamic and non-hemodynamic actions. Ginsenoside Rg5 (Rg5) occurs naturally in ginseng, which has shown various benefits for cardiovascular diseases. This study evaluated Rg5′s effects on Ang II-caused cardiac remodeling and heart failure. C57BL/6 mice developed hypertensive cardiac failure after four weeks of Ang II infusion. The mice were administered Rg5 via oral gavage for the last two weeks to investigate the potential mechanism of Rg5. RNA sequencing of heart tissues was performed for mechanistic studies. It was discovered that Rg5 inhibited cardiac inflammation, myocardial fibrosis, and hypertrophy, and prevented cardiac malfunction in mice challenged with Ang II, without altering blood pressure. RNA sequencing showed that Rg5′s cardioprotective effect involves the JNK/AP-1 signaling pathway. Rg5 diminished inflammation in mice hearts and cultured cardiomyocytes by blocking Ang II-activated JNK/AP-1 pathway. In the absence of JNK or AP-1 in cardiomyocytes, the anti-inflammatory effects of Rg5 were nullified. The study found that Rg5 preserved the hearts of Ang II-induced mice by reducing JNK-mediated inflammatory responses, suggesting that Rg5 is an effective therapy for hypertensive heart failure.

1. Introduction

Among adults, more than 30 percent have hypertension, making it a significant contributor to the prevalence of such devastating diseases as myocardial infarction, stroke, and heart failure [1]. A high concentration of angiotensin II (Ang II) activates the local renin-angiotensin system (RAS) and has detrimental consequences on the heart, containing cardiac remodeling and hypertrophy [2]. Ang II is a multifunctional cytokine that causes oxidative stress and inflammation, which damage the blood arteries and hearts [3]. Cardiomyocytes are induced to adopt an inflammatory phenotype by Ang II, which has been linked to cardiac fibrosis and remodeling, according to studies [4]. Because hypertension-targeting RAS blockers cannot completely reverse the cardiac remodeling and dysfunction in clinical management [5], from a non-hemodynamic perspective, it is beneficial to pursue drugs that can counteract the effects of Ang II, like Ang II-induced chronic inflammation.

Natural therapies have been used to treat and prevent diseases for millennia. Undoubtedly, Traditional Chinese medicine (TCM) is the safer treatment in modern medicine, while Ginseng has been used for a long time as a natural medicine, such as anti-cancer, anti-inflammation, anti-diabetes, anti-obesity, neuroprotection, and cardioprotection [6].

Abbreviations: Ang II, angiotensin II; AP-1, Activator Protein 1; CMC-Na, sodium carboxyl methylcellulose; Col-1, collagen type 1; FITC, Fluorescein Isothiocyanate; GAPDH, glyceraldehyde-3 phosphate dehydrogenase; IL-1β, interleukin 1beta; IL-6, interleukin 6; JNK, c-Jun N-terminal kinase; LV, left ventricular; MAPK, -activated protein kinase; MTT, methyl thiazolyl tetrazolium; NF-κB, nuclear factor-κB; RAS, renin-angiotensin system; Rg5, Ginsenoside Rg5; TGF-β, transforming growth factor β; TNF-α, tumor necrosis factor α; WGA, wheat germ agglutinin; β-MyHC, β-myosin heavy chain.

* Corresponding authors at: Affiliated Yongkang First People's Hospital and School of Pharmacy, Hangzhou Medical College, Hangzhou, Zhejiang 310012, China.
E-mail addresses: wzmcliangguang@163.com (G. Liang), 15643584357@163.com (M. Wang).

[1] These authors contributed equally to this work.

https://doi.org/10.1016/j.intimp.2023.110408
Received 20 April 2023; Received in revised form 21 May 2023; Accepted 28 May 2023

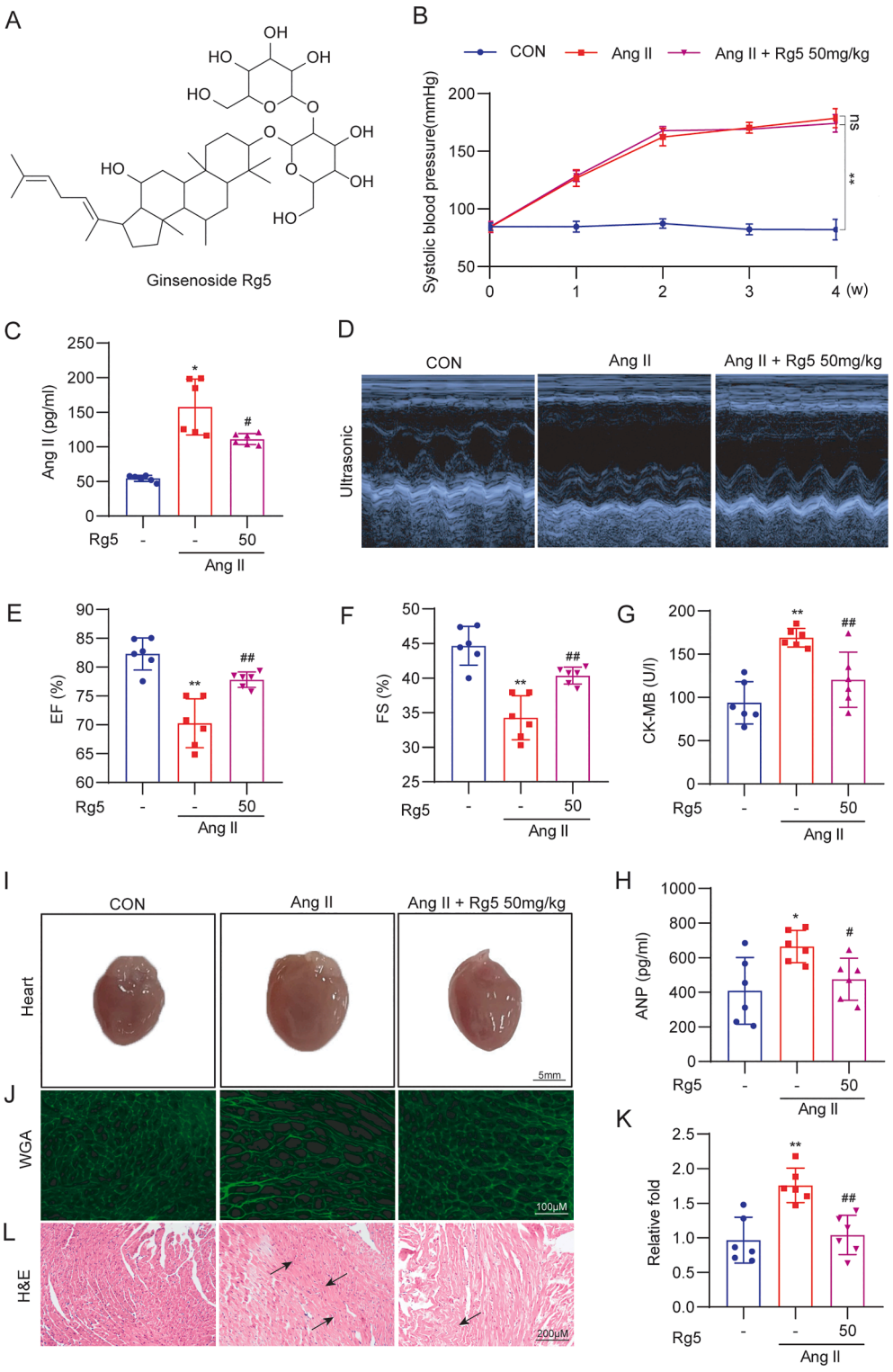

Fig. 1. Rg5 prevents Ang II-induced cardiac remodeling and dysfunction in mice. Mice were treated as described in Methods. **(A)** Chemical structure of Ginsenosides Rg5 (Rg5). **(B)** Periodic systolic blood pressure measurement as determined by non-invasive tail-cuff Pressure Analysis System weekly. **(C)** Ang II levels in mouse serum were determined by ELISA kit. **(D)** Cardiac function in mice was determined by noninvasive echocardiography. **(E-F)** EF and FS of mice measured by ultrasonic scanning image system. **(G-H)** CK-MB and ANP levels in mice serum were determined using Biochemical kit and ELISA kit respectively. **(I)** Representative fresh heart images in white background. **(J)** Representative wheat germ agglutinin (WGA) staining of heart tissues [scale bar = 100 μm]. **(K)** Quantitative analysis of myocyte area. A minimum of 100 cells were measured from different visual fields of 6 samples per group. **(L)** Representative hematoxylin-eosin (H&E) staining image of heart tissues [scale bar = 200 μm], black arrows indicating myocardial fiber arrangement disorder (n = 6, data were presented as mean ± SEM. $^{*}p < 0.05$, $^{**}p < 0.01$ vs. CON group; $^{\#}p < 0.05$, $^{\#\#}p < 0.01$ vs. Ang II-treated group).

Ginsenoside Rg5 (Rg5) has demonstrated excellent pathological effects, including anticancer, antiallergy, anti-inflammatory, immune-boosting, and hypoxia resistance, and a preventive role in cardiovascular diseases (CVDs) [7–9]. Rg5 (shown in Fig. 1A), a minor ginsenoside synthesized during steaming of ginseng, has better medicinal activities compared with major ginsenosides. Rg5 prevented cell apoptosis with increased HK-II binding and reduced Drp1 recruitment to mitochondria in isoproterenol-induced ischemic heart of mice [10]. Rg5 significantly inhibited hypoxia-induced NRMs apoptosis, decreased the expression pro-apoptotic protein Bax, increased the expression of anti-apoptotic protein Bcl-2 ratio and the level of cleaved caspase 3. Akt signaling activation was found to be the mechanism of Rg5′s protective effect on hypoxia-induced NRMs apoptosis, as an Akt inhibitor eliminated the anti-apoptotic effects of Rg5. Rg5 suppressed hypoxia-induced apoptosis in NRMs via activation of the Akt signaling [8]. However, the value of Rg5 in the treatment of hypertensive heart failure remains uncertain.

In the present work, cardioprotective characteristics of Rg5 in hypertension were studied. Rg5′s ability to diminish the activation of c-Jun

N-terminal kinase (JNK) and the resultant activator protein 1 (AP-1) prevented Ang II–induced cardiac inflammation, fibrosis, and hypertrophy both in vivo and in vitro. Thus, Rg5 was identified as a potential novel treatment drug for hypertensive heart failure due to our research.

2. Materials and methods

2.1. Reagents

The reagents and antibodies used in this study are listed in the Supplemental Table S1.

2.2. Cell culture

Immortalized rat cardiomyocyte-like H9c2 cell line was purchased from the Shanghai Institute of Biochemistry and Cell Biology (Shanghai, China). The H9c2 cells were cultured in Dulbecco's modified Eagle medium (DMEM, cat no.11995040, Gibco; Eggenstein, Germany), with 10% fetal bovine serum (cat no.14160063, Gibco; Eggenstein, Germany) and 1% penicillin/streptomycin in an incubator that was humidified and contained 5% carbon dioxide. The temperature was 37 degrees Celsius (Invitrogen; CA, USA). As was discussed earlier, the medium used to cultivate the cells was DMEM.

2.3. Animal experiment

18 six-week-old male C57BL/6 mice, weighing 16–17 g, were provided by the Animal Center of Wenzhou Medical University. All animal care and experimental procedures in this study were approved by the Wenzhou Medical University's Animal Policy and Welfare Committee (Approval Document No. wydw2021-1031). All animals were treated humanely, per the guidelines set by the National Institutes of Health (USA). Before beginning in vivo tests, mice were given at least two weeks to acclimatize to their surroundings. Mice were placed in a controlled setting with a 12:12 light/dark cycle and typical rodent food.

To promote hypertensive cardiac damage, as previously described, mice were infused with Ang II via a micro-osmotic pump (catalog number Alzet MODEL 1004, Alzet, CA) [11]. The pump supplied 1 ng/kg/min Ang II for four weeks after being implanted in the back of mice. After pump implantation, mice received 1 g/L neomycin in their drinking water to keep wound disinfection. As mentioned earlier, the systolic blood pressure was monitored weekly using telemetric blood pressure equipment and a tail cuff (BP-2010A, Softron Biotech, Tokyo, Japan) [12]. After starting Ang II treatment, mice received intragastric injections of Rg5 that had been dissolved in 0.5% CMC-Na solution two weeks later. Previous research served as the basis for the selection of the Rg5 dosage, which were set at 50 mg/kg/d [13,14]. The groups will be divided using randomization this time. Mice were separated into the following four groups at random: (i) non-treated animals given a 0.5% CMC-Na vehicle solution (CON, n = 6); (ii) Mice that had been injected with Ang II and were given a 0.5% CMC-Na vehicle solution (Ang II; n = 6); (iii) Mice injected with Ang II and given Rg5 at 50 mg/kg daily (Ang II + 50 mg/kg Rg5; n = 6).

During the duration of the animal experiment, all mice survived. After the investigation, animals were slaughtered under the influence of sodium pentobarbital. After killing, the cardiac tissues and blood were collected. The weight of the heart, total body mass, and tibia length were measured and recorded. Serum biomarkers, including Ang II, CK-MB, and ANP, were assessed using the commercial kits, respectively. For gene and protein expression investigations, the tissues of mouse heart were snap-frozen in liquid nitrogen, and for histological examination, they were treated with 4% paraformaldehyde.

2.4. Cardiac functional tests

Transthoracic echocardiography was used to measure noninvasively systolic and diastolic heart function in sedated mice a day before sacrifice. Under the influence of isoflurane, 18 mice underwent echocardiography analysis using the SONOS 5500 ultrasonography with a 15-MHz linear array ultrasound transducer (Philips Electronics, Amsterdam, Netherlands).

2.5. WGA-FITC staining

Frozen sections of cardiac tissue were used for the immunofluorescence staining procedure. Analysis of frozen tissue sections with a thickness of 5 μm was performed after a permeabilization step of 0.1% Triton X-100 for ten minutes, followed by a blocking step of bovine serum albumin (5%) for thirty minutes. At 37 degreesC, a 1:200 solution of WGA-FITC dye was applied and stained for 30 min. Images were captured using a Nikon fluorescent microscope at 40 × magnification (Nikon, Tokyo, Japan).

2.6. Heart histology

The cardiac tissues were immersed in paraffin and sliced to a thickness of 5 μm. The amount of collagen in the cardiac tissues was determined using the Sirius red, H&E, and Masson's trichrome staining. A light microscope at 200 × magnification was used to record the stained sections (Nikon, Tokyo, Japan). Image J (NIH) was utilized to quantify collagen deposition using a single-blinded approach.

2.7. Rhodamine phalloidin staining

After treatment, H9c2 cells were fixed in 4% paraformaldehyde, permeabilized in Triton X-100 solution (0.1%), and then stained with rhodamine-conjugated phalloidin at 50 ng/ml for 30 min in order to examine hypertrophic changes in the cells. DAPI was utilized as a staining for the cell nuclei at room temperature. For the purpose of observing and documenting immunofluorescence, an epifluorescence microscope manufactured by Nikon (400 × magnification; Tokyo, Japan: Nikon) was used.

2.8. Cell viability assay

Three thousand H9c2 cells per well were grown and cultured onto a 96-well plate overnight. These cells were then subjected to increasing concentrations of Rg5, including 0.1, 0.5, 1, 2.5, 5, 10, 20, 40, and 80 μM. The vehicle for the control cells was DMSO. Following an incubation period of 24 h, each well was supplemented with methyl thiazolyl tetrazolium (MTT). After incubating the cells for four hours, DMSO was added. SpectraMax M5 microplate reader recorded absorbance at 570 nm (Molecular Devices, CA, USA). The proportion of viable cells was compared to the control group.

2.9. RNA transcriptome sequencing

Purified total RNA of mouse heart tissues was extracted using the TRIzol reagent (Invitrogen, CA, USA) according to the manufacturer's guidelines. Using NanoDrop ND-1000, the amount and purity of RNA in each cardiac sample were measured (NanoDrop, DE). The integrity of the RNA was examined by a Bioanalyzer 2100 (Agilent, CA) and then validated by electrophoresis assay on a denaturated agarose gel. Utilizing Dynabeads Oligo (dT)25–61005 (Thermo Fisher, CA), poly (A) RNA is isolated from 1 μg total RNA. The magnesium RNA Fragmentation Module (NEB, cat. e6150, MA) was then utilized to fragment poly (A) RNA into small fragments. SuperScriptTM II reverse transcriptase was then used to convert the cleaved RNA fragments into cDNA (Invitrogen, cat. 1896649, CA, USA). As per the manufacturer guidelines, the sequencing analysis was completed using an Illumina NovaseqTM 6000. After the whole transcriptome generation, all transcripts' expression levels were quantified. mRNAs with differential expression were

Table 1
Biometric and Echocardiographic Measurements in Experimental Mice.

	CON	Continuous Ang II Pump Infusion	
			Rg5 (50 mg/kg)
	n = 6	n = 6	n = 6
EF, %	83.30 ± 2.77	70.27 ± 4.26**	77.83 ± 1.33##
FS, %	44.65 ± 2.81	34.26 ± 3.18**	40.35 ± 1.22##
LVIDd, mm	2.1 ± 0.26	3.08 ± 0.40**	2.77 ± 0.34
IVSD, mm	0.63 ± 0.08	0.7 ± 0.09	0.67 ± 0.05
PWD, mm	0.62 ± 0.08	0.68 ± 0.04	0.65 ± 0.05
E wave, m/s	0.67 ± 0.06	0.56 ± 0.05**	0.69 ± 0.07##
Tei Index	0.69 ± 0.17	0.77 ± 0.14	0.75 ± 0.08
IRT, ms	17.17 ± 5.53	16.67 ± 1.51	15.67 ± 3.01
HR, bpm	535.67 ± 22.16	522 ± 39.14	537 ± 20.73
HW/BW, mg/g	5.51 ± 0.26	6.21 ± 0.49*	5.67 ± 0.41#
HW/TL, mg/mm	6.11 ± 0.47	8.39 ± 0.54**	7.21 ± 0.73##

Transthoracic echocardiography was performed on mice at the end of the animal study. Ang II, angiotensin II; BW, body weight; CON, control; EF, ejection fraction; E wave, peak mitral E velocity; FS, fractional shortening; HR, heart rate; HW, heart weight; IRT, isovolumic relaxation time; IVSD, diastole interventricular septal thickness; LVIDd, diastole left ventricle internal dimension; PWD, diastole posterior wall thickness; Rg5, Ginsenoside Rg5; Tei index, a myocardial performance index designed by Dr. Chuwa Tei. Data presented as mean ± SEM. *$p < 0.05$, **$p < 0.01$ compared with CON group; #$p < 0.05$, ##$p < 0.01$ compared with Ang II Pump.

identified utilizing the following criteria: fold change < 0.5 or fold change greater than 2, with p-value < 0.05.

2.10. Real-time qPCR (RT-qPCR)

Using Trizol Reagent, total RNA was isolated from the cells or tissues. 1 μg total RNA was reverse-transcribed utilizing PrimeScriptTM RT reagent Kit (cat. no. DRR037A, Takara Bio Inc., Kusatsu, Japan). Using the CFX96 Touch Real-Time PCR Detection System, TB Green® Premix Ex TaqTM II (RR820B, Takara Bio Inc., Kusatsu, Japan) and particular primers were subsequently added and utilized for real-time qPCR assay (Bio-Rad; CA, USA). Normalization of the gene expression levels relative to that of the housekeeping gene β-actin. The primers used in this study were provided in Table S2 of the Supplement.

2.11. Western blot analysis

Using 10% SDS-PAGE, homogenates of the lysates of cells or tissues were divided and electrotransferred onto PVDF membranes. 1.5 h were spent blocking membranes in Tris-buffered saline, which contains Tween20 (0.05%) and non-fat milk (5%). Then, the specific primary antibodies were incubated with the PVDF membranes. Immunoreactive bands were observed using secondary antibodies coupled to improved chemiluminescence reagent and horseradish peroxidase (Bio-Rad; CA, USA). Using the 1.38e version Image J analysis software, densitometric measurements were standardized to their corresponding controls.

2.12. Statistical analysis

The GraphPad Prism v8.0 software (San Diego, CA) was utilized for statistical analysis. A one-way analysis of variance (ANOVA) was conducted, followed by a multiple comparisons test with Bonferroni correction. The outcomes are presented as the mean ± SEM and p-value < 0.05 was deemed substantial.

3. Results

3.1. Rg5 inhibits cardiac remodeling and dysfunction produced by Ang II infusion in mice

We first examined whether Rg5 prevents cardiac damage caused by Ang II in mice. As depicted in Fig. 1B, the systolic blood pressure was raised in mice with Ang II infusion, and the Rg5 therapy did not affect blood pressure. As anticipated, Ang II infusion boosted serum Ang II

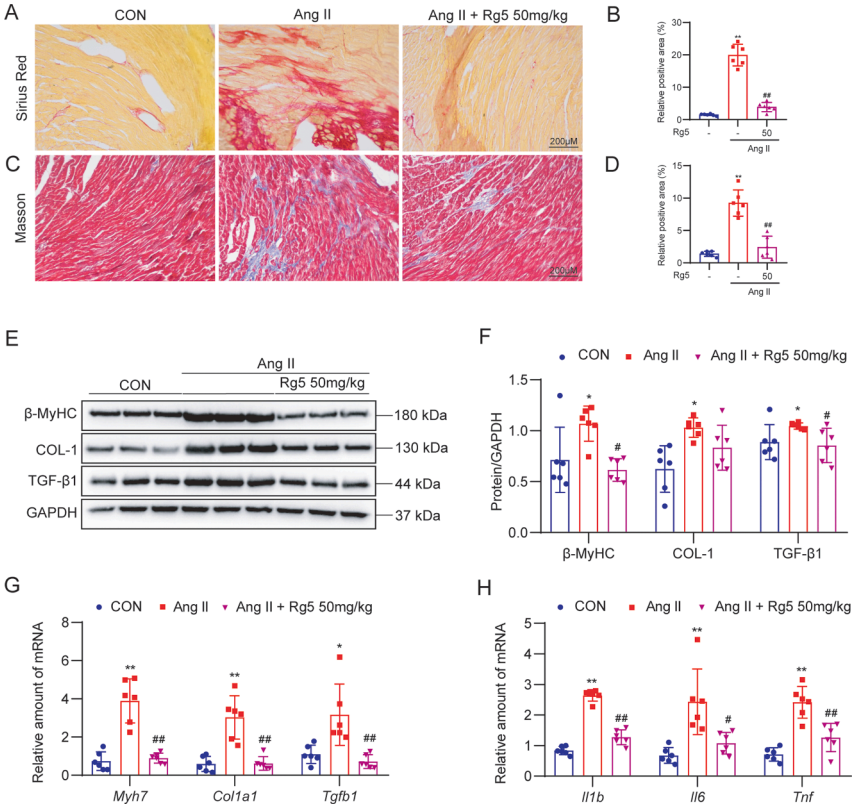

Fig. 2. Rg5 prevents Ang II-induced heart fibrosis and inflammation in mice. Mice were treated as described in Methods. **(A)** Representative micrographs of cardiovascular Sirius Red staining. **(B)** Quantification of Picro Sirius Red staining of heart tissues in plane A. **(C)** Representative micrographs of Masson trichrome staining. [scale bar = 200 μm]. **(D)** Quantification of Masson trichrome staining of heart tissues in plane C. **(E)** Representative Western blot analysis of β-MyHC, COL-1, and TGF-β1 in heart tissues. GAPDH was used as the loading control. **(F)** Quantitative data of the blot intensity of corresponding proteins determined by Image J software in plane E **(G)** The mRNA levels of *myh7*, *Col1a*, and *Tgfb1* were detected by RT-qPCR in the heart tissues. **(H)** The mRNA levels of *Il1b, Il6 and Tnf* were detected by RT-qPCR in the heart tissues. (n = 6, data were presented as mean ± SEM. *$p < 0.05$, **$p < 0.01$ vs. CON group; #$p < 0.05$, ##$p < 0.01$ vs. Ang II-treated group). (For interpretation of the references to color in this figure legend, the reader is referred to the web version of this article.)

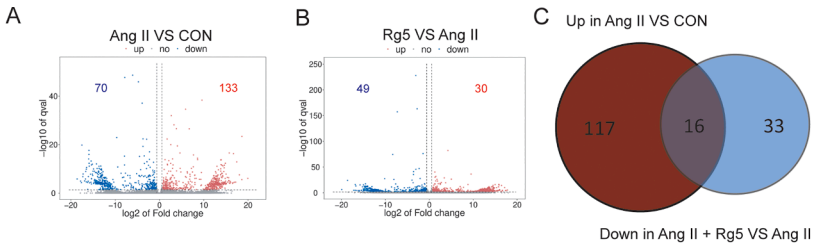

D

Bioplanet 2019	
Name	**P-value**
Wnt interactions in liqid metabolism and immune response	0.03541
Amino sugar and nucleotide sugar metabolism	0.03541
HNF3B pathway	0.03541
Syndecan 1 pathway	0.03619
Actions of nitric oxide in the heart	0.03696
Agrin in postsynaptic differentiation	0.03696
Myometrial relaxation and contraction pathways	0.00667
Amino acid and oligopeptide SLC transporters	0.03850
Type 2 diabetes mellitus	0.03927
JNK/MAPK pathway	0.04158

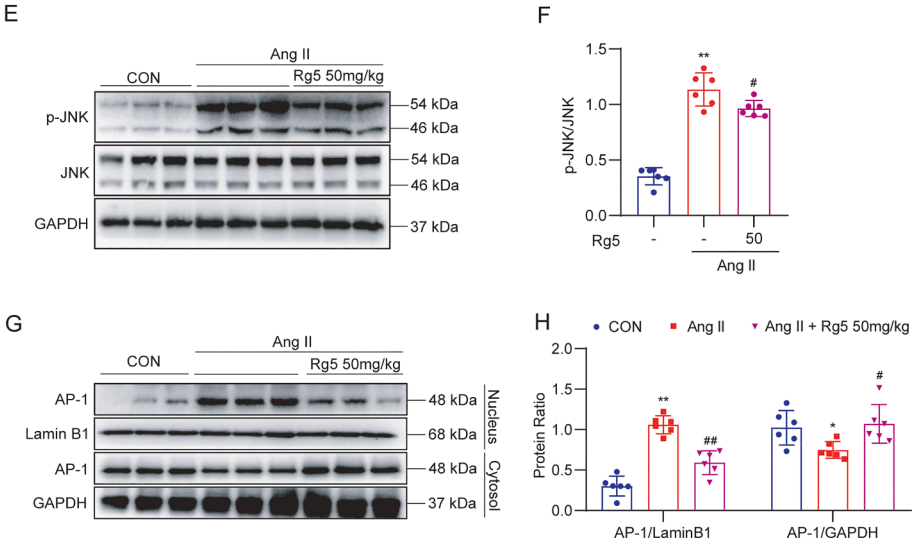

Fig. 3. The cardioprotection of Rg5 is associated with inhibiting JNK and AP-1. Mice were treated as described in Methods. **(A-B)** Volcano map of differentially expressed genes between Ang II-treated group and control group (A); Volcano map of differentially expressed genes between Ang II-treated group and Rg5 pretreatment + Ang II-treated group (B); Red color indicates upregulation of genes while blue color indicates downregulation, and the grey color in the middle were the genes have no difference. **(C)** Venn diagram of up-regulated genes of in Ang II-treated group vs control group and Ang II-treat group vs Rg5 pretreatment + Ang II-treated group. **(D)** The list of BioPlanet 2019 pathway analysis followed by expression analysis of intersecting genes in plane C. **(E)** Representative Western blot analysis of p-JNK and JNK in the heart tissues. GAPDH was used as the loading control. **(F)** Quantitative data of the blot intensity of corresponding proteins determined by Image J software in plane E. **(G)** Representative Western blot analysis of AP-1 in the heart tissues. GAPDH and Lamin B1 was used as the loading control. **(H)** Quantitative data of the blot intensity of corresponding proteins determined by Image J software in plane G. (n = 6, data were presented as mean ± SEM. $^{*}p < 0.05$, $^{**}p < 0.01$ vs. CON group; $^{\#}p < 0.05$, $^{\#\#}p < 0.01$ vs. Ang II-treated group). (For interpretation of the references to color in this figure legend, the reader is referred to the web version of this article.)

concentrations. However, Rg5 did not affect this increase in mice (Fig. 1C). These outcomes demonstrate that Rg5 is devoid of hypotensive properties. Intriguingly, noninvasive echocardiography revealed that Rg5 ameliorated Ang II–induced heart dysfunction, as demonstrated primarily by the reversal of fractional shortening (FS) and ejection fraction (EF) percentage values in Rg5-treated hypertensive mice (Fig. 1D–F, and Table 1). Moreover, medication with Rg5 reduced serum CKMB and ANP levels in Ang II-treated animals (Fig. 1G–H). Next, we evaluated Rg5′s influence on heart morphological deterioration. Gross examination and WGA staining revealed hypertrophic alterations in hearts of Ang II-challenged mice, whereas Rg5 significantly decreased cardiac hypertrophy in Ang II-challenged mice (Fig. 1I–K). Comparable outcomes were seen when comparing mice's heart weight/tibia length and heart weight/body weight ratios (Table 1). Ang II-induced histological alterations in the hearts of mice treated with Rg5-showed considerable improvement when examined with H&E staining, which revealed these modifications (Fig. 1L). Based on these results, Rg5 proved to be highly effective in shielding the hearts of study mice from the hypertrophy and functional impairment that are typically caused by Ang II.

3.2. *Rg5 protects mice against Ang II-induced cardiac inflammation and fibrosis*

Heart inflammation and fibrosis are examined in mice. We found that Rg5 remarkably inhibits Ang II-induced cardiac fibrosis as evidenced by Masson's trichrome staining and Sirius Red staining (Fig. 2A–D). The cardiac fibrosis and hypertrophy in Ang II-infused mice were further confirmed by elevated β-MyHC, TGF-β1, and COL-1 protein and mRNA levels. These changes were significantly reversed by Rg5 therapy (Fig. 2E–G). In addition, the mRNA levels of inflammatory genes including interleukin 1β (*Il1b*), interleukin 6 (*Il6*), and tumor necrosis factor (*Tnf*) were dramatically elevated in the Ang II-infused mice's hearts, while administration of Rg5 almost completely reversed these increases (Fig. 2H).

3.3. *The cardioprotection of Rg5 is associated with JNK and AP-1 inhibition*

We sequenced the RNA extracted from the hearts of mice to explore the probable mechanism by which Rg5 protects the heart from the damage caused by Ang II. There were a total of 203 genes in the Ang II-challenged group that were significantly different from those in the control mice, with 133 upregulated and 70 downregulated (Fig. 3A).

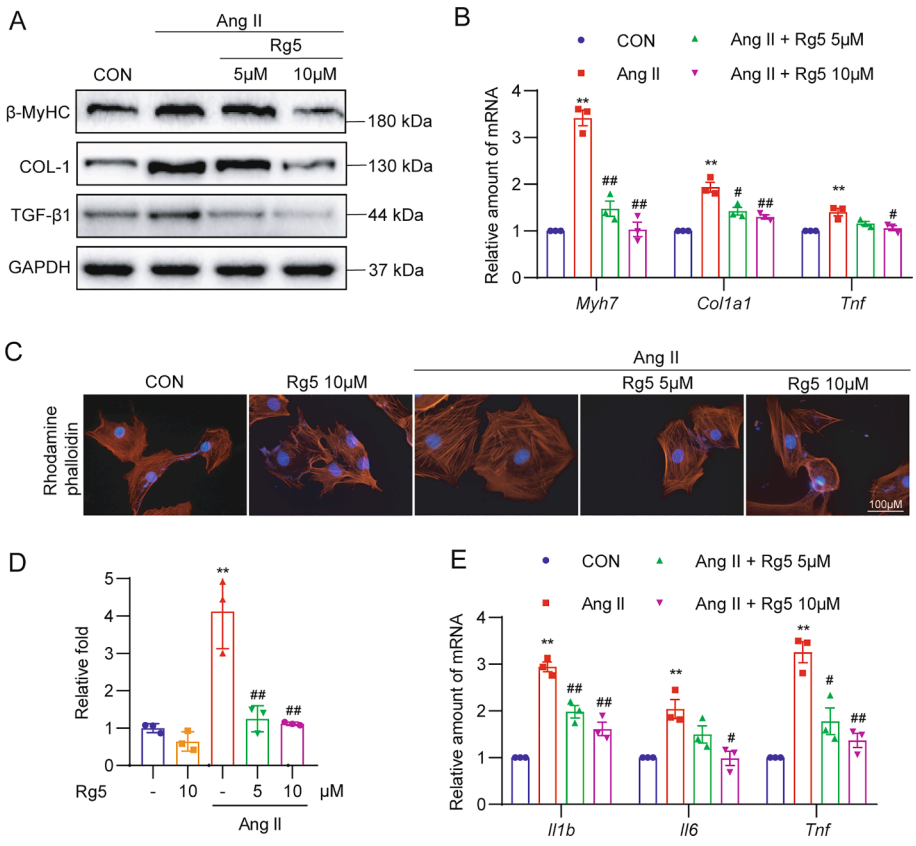

Fig. 4. Rg5 prevents Ang II-induced hypertrophy, fibrosis, and inflammation in H9c2 cells. H9c2 cells were pretreated with 5 or 10 μM Rg5 for 1 h and then exposed to Ang II (1 μM) for 8 or 24 h. Protein and RNA were extracted to perform immunoblotting and qPCR respectively. **(A)** Representative Western blot analysis of β-MyHC, COL-1 and TGF-β1 in the H9c2 cells. GAPDH was used as the loading control. **(B)** RT-qPCR showing mRNA levels of *myh7*, *Col1a* and *Tgfb1* in the H9c2 cells. **(C)** TRITC phalloidin (red) staining of H9c2 cells showing the effect of Rg5 on Ang II-induced hypertrophic responses. Slides were counterstained with DAPI (blue). **(D)** Quantification of cell size increase in H9c2 cells in response to Ang II and the effect of Rg5 on such increases. A minimum of 100 cells were measured from different visual fields of 3 samples per group [scale bar = 100 μm]. **(E)** RT-qPCR showing mRNA levels of *Il1b*, *Il6*, and *Tnf* in the H9c2 cells. (n = 3, data were presented as mean ± SEM. $^{*}p < 0.05$, $^{**}p < 0.01$ vs. CON group; $^{\#}p < 0.05$, $^{\#\#}p < 0.01$ vs. Ang II group). (For interpretation of the references to color in this figure legend, the reader is referred to the web version of this article.)

Furthermore, there were a total of 79 genes in the Rg5 + Ang II group that were significantly different from those in the control mice with 30 upregulated and 49 downregulated (Fig. 3B). Sixteen genes were found to be controlled by Rg5 in the Ang II environment (Fig. 3C). Analysis of the expression of these 16 genes using BioPlanet 2019 revealed the probable participation of the JNK/ MAPK pathway (Fig. 3D). The MAPK signaling pathway has been considered to be critical for controlling inflammation[15]. JNK belongs to the MAPK family and is triggered by a variety of ambient stressors, growth regulators, and inflammatory cytokines. It has been suggested that JNK activation contributes to hypertensive heart failure[16]. In addition, Western blot assay indicated that JNK phosphorylation was elevated in the hearts of Ang II-challenged mice. At the same time, Rg5 therapy dramatically decreased JNK phosphorylation in the hearts (Fig. 3E–F). Immunoblotting was done to examine if Rg5 influenced Ang II-induced activation of AP-1. Ang II stimulation increased AP-1 nuclear translocation in the hearts of wild-type mice, whereas Rg5 abolished this effect dose-dependently (Fig. 3G–H).

3.4. Rg5 protects H9c2 cells from Ang II-induced fibrosis, hypertrophy, and inflammation

As a cellular model to evaluate if Rg5 cardioprotection is achieved by direct targeting of cardiomyocytes, H9c2 cells were employed. According to a methyl thiazolyl tetrazolium test, Rg5 concentrations ranging from 0.1 to 80 μM were not harmful to H9c2 cells (Supplementary Figure S1). Rg5 suppressed Ang II-increased mRNA and protein expression of β-MyHC, TGF-β1, and COL-1 in a dose-dependent manner, as shown by western blotting and quantitative RT-qPCR (Fig. 4A–B and Supplementary Figure S2). Rg5 also blocks Ang II-induced hypertrophy of H9c2 cells, as shown by rhodamine phalloidin labeling (Fig. 4C–D). Moreover, RT-qPCR assay demonstrated that Ang II enhanced the mRNA expression of inflammatory genes *Tnf, Il1b*, and *Il6* in H9c2 cells, whereas Rg5 significantly prevented these alterations (Fig. 4E). These findings imply that Rg5 inhibits the hypertrophy, fibrosis, and inflammation caused by Ang II in cardiomyocytes.

3.5. Rg5 protects cardiomyocytes by inhibiting JNK/AP-1 activation

Then, we investigated whether the cardioprotective effects of Rg5 are related to JNK suppression in H9c2 cells activated by Ang II. Immunoblot analysis of the JNK pathway revealed enhanced phosphorylation of JNK in Ang II-treated H9c2 cells. However, p-JNK levels were significantly reduced by Rg5 therapy (Fig. 5A-B). As seen in Fig. 5C–H, treatment with the JNK inhibitor decreased the Ang II-induced mRNA expression of pro-inflammatory (*Tnf, Il6, and Il1b*), pro-fibrotic (*Col1a1* and *Tgfb1*), and pro-hypertrophic (*Myh7*) genes in H9c2 cardiomyocytes. SP600125′s suppression of JNK removed the intrinsically preventative effects of Rg5 on Ang II-induced mRNA expression of indicated genes (Fig. 5C–H). We then confirmed that AP-1 nuclear translocation was also inhibited following JNK inhibition by measuring the nuclear AP-1 levels in the H9c2 cells (Fig. 5I–J). These findings indicate that Rg5 suppresses JNK to prevent Ang II-induced cardiomyocyte damage.

4. Discussion

This work demonstrated that therapy with Rg5 prevents hypertensive heart failure by suppressing the JNK/AP-1-mediated cardiac inflammation. In a mouse model challenged by Ang II, Rg5 decreased heart fibrosis and hypertrophy and reduced cardiac dysfunction. The Rg5 therapy effectively reduced Ang II's activation of JNK/AP-1 in mouse hearts and cultured cardiomyocytes. The pathological damages caused by Ang II and the pharmacological effects of Rg5 were reduced when MAPK was suppressed using commercially available small-molecule inhibitors. According to these findings, Rg5 is a promising

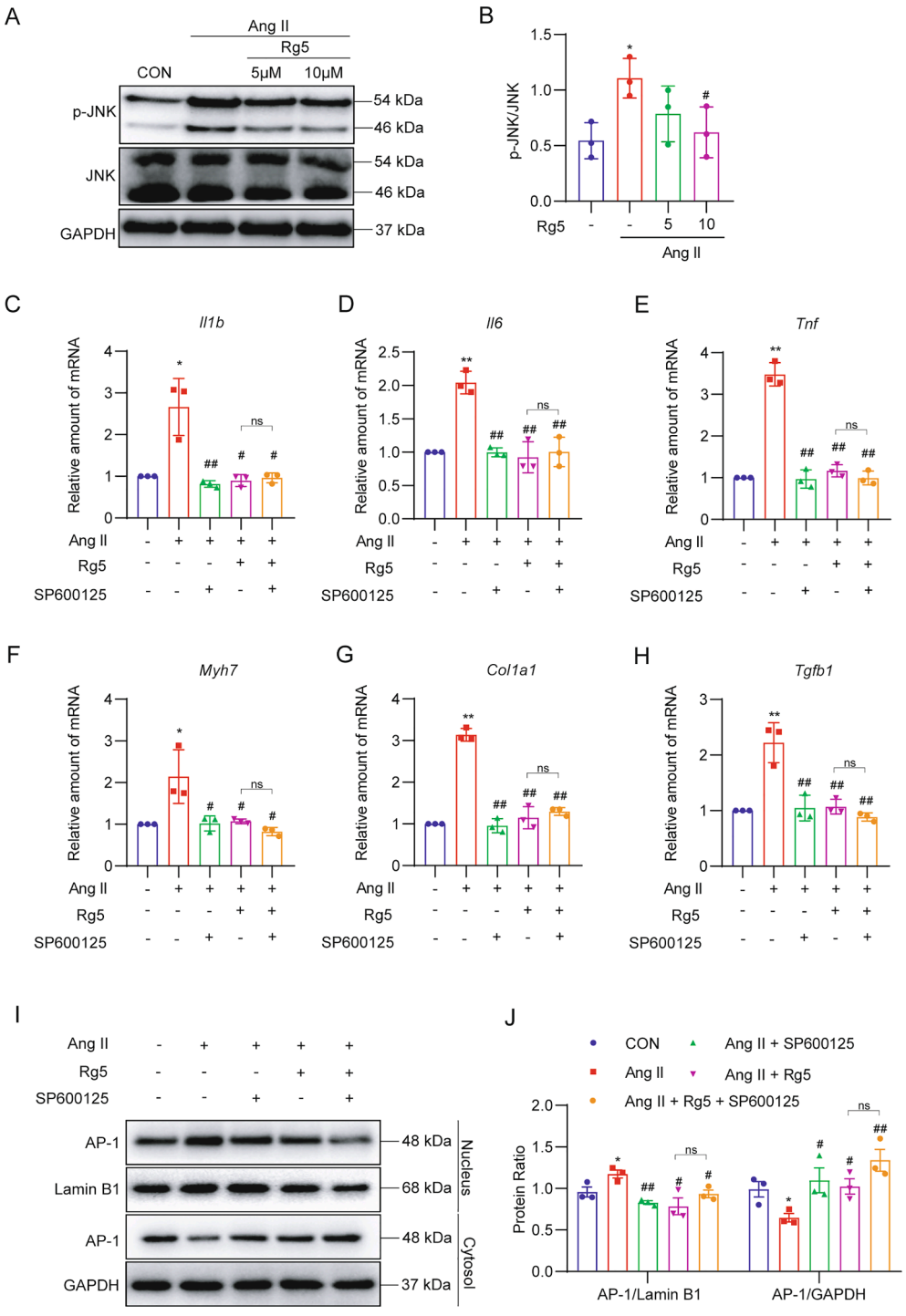

Fig. 5. Rg5 protects cardiomyocytes through inhibiting AP-1 and JNK signaling pathway activation. H9c2 cells were pretreated with 5 μM or 10 μM Rg5 with or without the presence of SP-600125 (5 μM, SP-600125: JNK inhibitor). After 1-h pre-treatment, cells were exposed to Ang II (1 μM) for 2 h. Then RNA and protein were extracted to perform immunoblotting and qPCR respectively. **(A)** Representative Western blot analysis of p-JNK, JNK in the H9c2 cells. GAPDH was used as the loading control. **(B)** Quantitative data of the blot intensity of corresponding proteins determined by Image J software in plane A. **(C-E)** RT-qPCR showed the mRNA levels of inflammatory factors (*Il1b, Il6, and Tnf*) in H9c2 cells. **(F-H)** RT-qPCR showed the mRNA levels of fibrosis-related genes (*β-MyHC, COL-1 and TGF-β1*) in H9c2 cells. (n = 3, data were presented as mean ± SEM. $^{*}p < 0.05$, $^{**}p < 0.01$ vs. CON group; $^{\#}p < 0.05$, $^{\#\#}p < 0.01$ vs. Ang II-treated group). **(I)** Representative Western blot analysis of AP-1 in the H9c2 cells. GAPDH was used as the loading control. **(J)** Quantitative data of the blot intensity of corresponding proteins were determined by Image J software in plane I.

drug choice for treating hypertensive heart failure, and JNK and AP-1 are prospective targets for decreasing cardiac inflammation and pathological remodeling. The key findings of the current study are depicted graphically in Graphic Abstract.

Blood pressure control is an effective therapy for hypertensive cardiac remodeling, a globally significant cause of cardiovascular mortality. However, no effective medication exists to slow the growth of cardiac enlargement and fibrosis. In a pig model, dapagliflozin may slow the progression of left ventricular (LV) concentric hypertrophy by suppressing the inflammatory reaction[17]. Here, we discovered that Rg5, a ginsenoside, might lessen the aforementioned negative qualities without influencing blood pressure. Rg5 has anti-inflammatory properties that protect mice hearts against pathological remodeling caused by cardiac fibrosis and hypertrophy. Recently, some ginsenosides, such as ginsenoside Rg3, ginsenoside Rb1 and ginsenoside Rg2, avoiding myocardial fibrosis and hypertrophy induced by Ang II has also been demonstrated [18–20]. Thus, ginsenosides may serve as a source of treatment for heart failure caused by Ang II.

Ginseng is a common herbal remedy that has been found to have several medicinal effects. Rg5 has substantial potential activity for use as a broad-spectrum anticancer and anti-inflammatory drug. Rg5 has been reported to exert several positive effects on the nervous system, which potentiate the clinical applications of Rg5 in the treatment of neurodegenerative diseases. Additional studies have investigated other

pharmacological properties, such as cardioprotective, anti-OA, anti-OP, antidiabetic and anti-obesity effects [6]. Recent research indicates that Rg5 may ameliorate renal injury by regulating c-jun and then alleviating inflammation and apoptosis[18]. Morever, Rg5 acts primarily by targeting the NF-κB, TGF-β/Smad, PI3K/Akt/mTOR, and JNK pathways to reduce pneumonia, fibrosis, and suppress tumor progression, resulting in improved respiratory disease[19]. Rg5 is a minor ginsenoside synthesized during ginseng steaming treatment that exhibits superior pharmaceutical activity compared with major ginsenosides. Rg5 has the potential to act as a potential therapeutic candidate for diverse diseases [6]. To our knowledge, the present investigation was the first to demonstrate that Rg5 significantly suppressed cardiac remodeling and dysfunction caused by Ang II by exerting an anti-inflammatory effect.

One of the intersecting pathways is the JNK/MAPK signaling pathway, as revealed by our RNA-sequencing data. The JNK signaling pathway is implicated in several diseases, from cancer to neurological and immunological/inflammatory disorders [20]. JNK kinases have been involved in various cardiomyocyte development and fibrosis-related pathways. JNK activation is raised in failing human hearts [21], and the expression of MLK, an upstream JNK activator, is elevated in individuals with end-stage heart failure[22]. Experiments revealed that Ang II enhanced phosphorylated JNK activation in cardiac tissue and cultured cardiomyocytes, substantially reduced by Rg5 therapy. JNK inhibition by SP600125 reversed Rg5′s effects on cardiomyocytes, demonstrating that JNK regulates the cardioprotective and anti-inflammatory actions of Rg5.

We concentrated on the putative transcriptional component involved in the cardioprotective activities of Rg5. AP-1 is a canonical transcriptional factor downstream of JNK. Following phosphorylation by kinases such as PI3K/Akt and JNK, the transcriptional factor AP-1 translocates to nuclei from the cytosol to regulate target gene expression [23,24]. AP-1 has been reported to directly regulate the heart fibrosis-related genes (such as *Tgfb1* and *Col1*) that exhibit a fetal phenotype[25]. Studies have shown that transient activation of AP-1 transcription factors enhances cardiomyocyte development in response to numerous stimuli, including fatty acid and adrenergic signals[26]. In wild-type mice, we discovered that Ang II boosted AP-1 nuclear translocation but that Rg5 could counteract this effect. The same pattern of findings was seen in cultured cardiomyocytes. Ang II-induced AP-1 overexpression was substantially attenuated by inhibition of JNK with either Rg5 or SP600125. Based on these findings, we know that Ang II activates the JNK/AP-1 axis, leading to cardiac hypertrophy and fibrosis.

Rg5 may protect the heart by modulating signaling pathways other than the JNK/AP-1 axis. Recent research has connected these pathways to the etiology of hypertensive heart failure. Research is needed to evaluate the relative importance of each route in explaining the pharmacological actions of Rg5. Additionally, further research is needed to elucidate the direct interaction between Rg5 and JNK or to demonstrate the molecular targets by which Rg5 suppresses JNK activation. In conclusion, inhibition of JNK-mediated cardiac inflammation by Rg5 is reported to safeguard the heart in Ang II-induced hypertension mice, suggesting Rg5 as a treatment possibility for hypertensive heart failure.

CRediT authorship contribution statement

Tianxiang Yu: Data curation, Software. **Xiangwei Xu:** Investigation, Methodology. **Jiajia Wei:** Conceptualization, Data curation. **Jiachen Xu:** Resources, Software. **Wu Luo:** Validation, Supervision, Funding acquisition. **Ankang Li:** Visualization. **Guang Liang:** Writing-review & editing, Funding acquisition. **Mengyang Wang:** Writing-original draft.

Declaration of Competing Interest

The authors declare that they have no known competing financial interests or personal relationships that could have appeared to influence the work reported in this paper.

Data availability

Data will be made available on request.

Acknowledgements

The National Natural Science Foundation of China provided funding for this research. (82000793 to W.L., 21961142009 to G.L.).

Guang Liang and Mengyang Wang assisted in the literature review and the design of the study. Mengyang Wang contributed to the article's writing. The experiments were conducted by Tianxiang Yu, Xiangwei Xu, Jiajia Wei, Jiachen Xu. Guang Liang and Mengyang Wang were responsible for revising the text. Wu Luo and Ankang Li assisted in the collecting and processing of data. No paper mill was utilized, as all data were created in-house. All authors agree to be responsible for all elements of the work's accuracy and integrity.

Appendix A. Supplementary data

Two figures and two tables are provided as appendices. Any more information can be obtained upon request from the authors. Supplementary data to this article can be found online at https://doi.org/10.1016/j.intimp.2023.110408.

References

[1] A.E. Dikalova, A. Pandey, L. Xiao, L. Arslanbaeva, T. Sidorova, M.G. Lopez, F.T. t. Billings, E. Verdin, J. Auwerx, D.G. Harrison, S.I. Dikalov, Mitochondrial Deacetylase Sirt3 Reduces Vascular Dysfunction and Hypertension While Sirt3 Depletion in Essential Hypertension Is Linked to Vascular Inflammation and Oxidative Stress, Circ Res 126 (2020) 439–452.

[2] V. Sepulveda-Fragoso, B. Alexandre-Santos, A.C.P. Salles, A.B. Proenca, A.P. de Paula Alves, M. Vazquez-Carrera, A.C.L. Nobrega, E.D.C. Frantz, D.C. Magliano, Crosstalk between the renin-angiotensin system and the endoplasmic reticulum stress in the cardiovascular system: Lessons learned so far, Life Sci 284 (2021), 119919.

[3] A. Montezano, A. Nguyen Dinh Cat, F. Rios, R. Touyz, Angiotensin II and vascular injury, Current Hypertension Reports 16 (2014) 431.

[4] J. Wu, E. Dong, Y. Zhang, H. Xiao, The Role of the Inflammasome in Heart Failure, Front. Physiol. 12 (2021), 709703.

[5] L. Arendse, A. Danser, M. Poglitsch, R. Touyz, J. Burnett, C. Llorens-Cortes, M. Ehlers, E. Sturrock, Novel Therapeutic Approaches Targeting the Renin-Angiotensin System and Associated Peptides in Hypertension and Heart Failure, Pharmacol. Rev. 71 (2019) 539–570.

[6] M. Liu, F. Liu, Y. Gao, J. Yin, W. Yan, J. Liu, H. Li, Pharmacological activities of ginsenoside Rg5 (Review), Exp. Ther. Med. 22 (2021) 840.

[7] A. Panossian, S. Abdelfatah, T. Efferth, Network Pharmacology of Ginseng (Part II): The Differential Effects of Red Ginseng and Ginsenoside Rg5 in Cancer and Heart Diseases as Determined by Transcriptomics, Pharmaceuticals (Basel, Switzerland) 14 (2021).

[8] C. Wang, C. Huang, J. Wang, J. Ye, Z. Xue, J. Zhang, Y. Ren, Ginsenoside Rg5 attenuates hypoxia-induced cardiomyocyte apoptosis via regulating theAkt pathway, Chem. Biol. Drug Design (2023).

[9] H. Heo, Y. Kim, B. Cha, S. Brito, H. Kim, H. Kim, B. Fatombi, S. Jung, S. Lee, L. Lei, S. Lee, G. Park, B. Kwak, B. Bin, J. Park, M. Lee, A systematic exploration of ginsenoside Rg5 reveals anti-inflammatory functions in airway mucosa cells, J. Ginseng Res. 47 (2023) 97–105.

[10] Y. Yang, J. Li, K. Liu, L. Zhang, Q. Liu, B. Liu, L. Qi, Ginsenoside Rg5 increases cardiomyocyte resistance to ischemic injury through regulation of mitochondrial hexokinase-II and dynamin-related protein 1, Cell Death Dis. 8 (2017) e2625.

[11] S. Ye, W. Luo, Z.A. Khan, G. Wu, L. Xuan, P. Shan, K. Lin, T. Chen, J. Wang, X. Hu, S. Wang, W. Huang, G. Liang, Celastrol Attenuates Angiotensin II-Induced Cardiac Remodeling by Targeting STAT3, Circ Res 126 (2020) 1007–1023.

[12] L. Wang, Y.L. Li, C.C. Zhang, W. Cui, X. Wang, Y. Xia, J. Du, H.H. Li, Inhibition of Toll-like receptor 2 reduces cardiac fibrosis by attenuating macrophage-mediated inflammation, Cardiovasc. Res. 101 (2014) 383–392.

[13] D. Xu, C. Wang, W. Zhao, S. Gao, Z. Cui, Antidepressant-like effects of ginsenoside Rg5 in mice: Involving of hippocampus BDNF signaling pathway, Neurosci. Lett. 645 (2017) 97–105.

[14] Y. Zhu, H. Yang, J. Deng, D. Fan, Ginsenoside Rg5 Improves Insulin Resistance and Mitochondrial Biogenesis of Liver via Regulation of the Sirt1/PGC-1α Signaling Pathway in db/db Mice, J. Agric. Food Chem. 69 (2021) 8428–8439.

[15] S. Alam, Q. Liu, S. Liu, Y. Liu, Y. Zhang, X. Yang, G. Liu, K. Fan, J. Ma, Up-regulated cathepsin C induces macrophage M1 polarization through FAK-triggered p38 MAPK/NF-κB pathway, Exp. Cell Res. 382 (2019), 111472.

[16] S. Craige, K. Chen, R. Blanton, J. Keaney, S. Kant, JNK and cardiometabolic dysfunction, Biosci. Rep. 39 (2019).
[17] N. Zhang, B. Feng, X. Ma, K. Sun, G. Xu, Y. Zhou, Dapagliflozin improves left ventricular remodeling and aorta sympathetic tone in a pig model of heart failure with preserved ejection fraction, Cardiovasc. Diabetol. 18 (2019) 107.
[18] J. Park, P. Choi, T. Kim, H. Ko, H. Kim, K. Kang, J. Ham, Protective Effects of Processed Ginseng and Its Active Ginsenosides on Cisplatin-Induced Nephrotoxicity. In Vitro and in Vivo Studies, J. Agric. Food Chem. 63 (2015) 5964–5969.
[19] L. Ding, H. Qi, Y. Wang, Z. Zhang, Q. Liu, C. Guo, J. Liu, Z. Chen, J. Li, J. Chen, Q. Huang, D. Zhao, Z. Wang, X. Li, Recent advances in ginsenosides against respiratory diseases: Therapeutic targets and potential mechanisms, Biomed. Pharmacotherapy = Biomed. Pharmacotherapie 158 (2023), 114096.
[20] K. Sabapathy, Role of the JNK pathway in human diseases, Prog. Mol. Biol. Transl. Sci. 106 (2012) 145–169.
[21] S. Cook, P. Sugden, A. Clerk, Activation of c-Jun N-terminal kinases and p38-mitogen-activated protein kinases in human heart failure secondary to ischaemic heart disease, J. Mol. Cell. Cardiol. 31 (1999) 1429–1434.
[22] T. Calamaras, R. Baumgartner, M. Aronovitz, A. McLaughlin, K. Tam, D. Richards, C. Cooper, N. Li, W. Baur, X. Qiao, G. Wang, R. Davis, N. Kapur, R. Karas, R. Blanton, Mixed lineage kinase-3 prevents cardiac dysfunction and structural remodeling with pressure overload, American J. Physiol. Heart Circulatory Physiol. 316 (2019) H145–H159.
[23] W. Dong, Y. Li, M. Gao, M. Hu, X. Li, S. Mai, N. Guo, S. Yuan, L. Song, IKKα contributes to UVB-induced VEGF expression by regulating AP-1 transactivation, Nucleic Acids Res. 40 (2012) 2940–2955.
[24] H. Menden, S. Welak, S. Cossette, R. Ramchandran, V. Sampath, Lipopolysaccharide (LPS)-mediated angiopoietin-2-dependent autocrine angiogenesis is regulated by NADPH oxidase 2 (Nox2) in human pulmonary microvascular endothelial cells, J. Biol. Chem. 290 (2015) 5449–5461.
[25] M. Karin, The regulation of AP-1 activity by mitogen-activated protein kinases, Philos. Trans. Roy. Soc. London Series B, Biol. Sci. 351 (1996) 127–134.
[26] H. Zhang, L. Pei, Z. Ouyang, H. Wang, X. Chen, K. Jiang, S. Huang, R. Jiang, Y. Xiang, K. Wei, AP-1 activation mediates postnatal cardiomyocyte maturation, Cardiovasc. Res. (2022).